Scaling relation for a compact crumpled thin sheet

Wubin Bai, Yen-Chih Lin, Tzon-Kun Hou, and Tzay-Ming Hong
Department of Physics, National Tsing Hua University, Hsinchu 300, Taiwan, Republic of China
(Dated: August 16, 2010)

A high-pressure chamber was designed to study the crumpling of thin sheets beyond the power-law regime. Preceded by a smooth transition, the crumpled ball that characterizes the high-pressure state contains less than 50% air and exhibits separate ordered domains. All the data for different sheet thickness, size, and even number collapse to a master line when using volume ratio and pressure as the plotting parameters. This suggested the existence of a scaling relation, which was ascribed to the emergence of the ordered structure. We proposed a mean-field bundled-layer model that explained the experimental findings well. Possible bearings on the granular and colloidal systems are discussed, where ordering can also be promoted when the rheology changes upon shearing.

PACS numbers: 46.32.+x, 62.20.F-, 89.75.Fb

Crumpling[1] is a ubiquitous phenomenon that can be found at all length scales, from the microscopic packing of DNA inside the tiny capsule of a virus and squeezing of blood cells in and out of our body issues to the crushing of aluminum cans and plastic bottles in our daily recycling. At a larger scale, the unwanted deformation of automobiles during car accidents and the plate tectonics which create mountains and canyons are also notable examples. In spite of its commonplace, many complex properties of crumpling are still under active investigations[2, 3]. One important question is how it remains so hard while most of its interior is empty with air. The other is the origin of the power-law behavior[4–7] between the ball radius R and the compression force F. Numerical simulations showed that under the condition, Föppl – von Kármán number $\gamma = K_0R_0^2/\kappa \propto (R_0/h_0)^2 \to \infty$ (where K_0 is the two-dimensional Young's modulus, R_0 is the initial radius, κ is the bending rigidity, and h_0 is the thickness of the thin sheet), the self-avoidance of the thin sheet played an important role in the crumpling process and

$$\frac{R}{R_0} = C(\frac{K_0R_0^2}{\kappa})^{\beta}(\frac{\kappa}{FR_0})^{\alpha}. \quad (1)$$

This implies that $R \propto R_0^{\nu}F^{-\alpha}$ where ν and α are expected to be universal for phantom ($\nu = 3/4$, $\alpha = 3/8$) and self-avoiding ($\nu = 4/5$, $\alpha = 1/4$) membranes.

Recent studies[8, 9] suggested that there existed a transition at high pressure beyond which the power-law behavior was replaced by a locked state. The X-ray tomography[10, 11] also provided us with a vast knowledge of the internal structure of a crumpled ball. It is the goal of this Letter to integrate our experience and experimental techniques to elucidate the nature of this pressure-induced transition and the new state that ensues. Since the X-ray studies already told us that the numerous layers inside the crumpled ball would have been aligned and bundled into separate domains, how and why this ordered structure leads to a different mechanical response from the power law will be invaluable to other systems, such as the granular materials[12], that exhibit a similar partial ordering at high packing ratio.

The high-pressure chamber shares the same crumpling mechanism with the version in Ref.[9]. The schematic experimental setup is shown in Fig.1. This system mainly consists of a steel chamber with acrylic windows on both sides for observation, a thin layer of plastic film to wrap the sample, and a steel tube connecting the sample to the outside. When the highly condensed nitrogen gas flows into the chamber, the pressure difference between the inner and outer side of the plastic film compresses the sample with an isotropic force. The thin film we adopted is latex, which is commonly used to produce condoms and ideal for preventing leakage of fluids. To monitor the leakage of the wrap, a flow-gauge is mounted on the tube that connects to the sample, as in Fig.1. The chamber has been tested to be capable of crumpling at 120 Pa with a leakage flow rate of about 71.7 ml/hr. To our knowledge, this design holds the highest record of pressure in isotropic crumpling. To achieve an even higher pressure, the gas shall have to be replaced by liquid. How to incorporate this to our design of pressure chamber will be a perspective challenge for us in the future.

During the crumpling process, we use a camera with a 3008×2000-pixel resolution to monitor the ball radius under different pressure. Since the pressure performed in this Letter covers a wide range, we use two gauges to measure its magnitude in different regions, 10^5 to 2×10^6 Pa and 1.5×10^5 to 1.2×10^7 Pa. Both gauges were calibrated to exhibit a coherent measurement in their overlapped range, but the low-pressure gauge allows a finer tuning. Aluminum foil and HDPE film of various dimensions and thicknesses h_0 are used. A list of samples is shown in Table 1. Each data point reported here was obtained from averaging 20 rounds of measurements.

To understand the mechanical resistance of a crumpled thin sheet under high pressure, we first use an aluminum foil of $h_0 = 16\mu$m and R_0=0.15m×0.15m. To follow the protocol of plot scale in previous works, the R/R_0-F relation is plotted in the inset of Fig.2. The radius R of the crumpled ball decreases with the applied force in a power-law fashion after the precrumple stage, as reported in [9]. When the applied force approaches ∼100 kgw, R starts to deviate from the power-law fitting and exhibits a slower decreasing rate. Since the applied force, $F = P \times 4\pi R^2$,

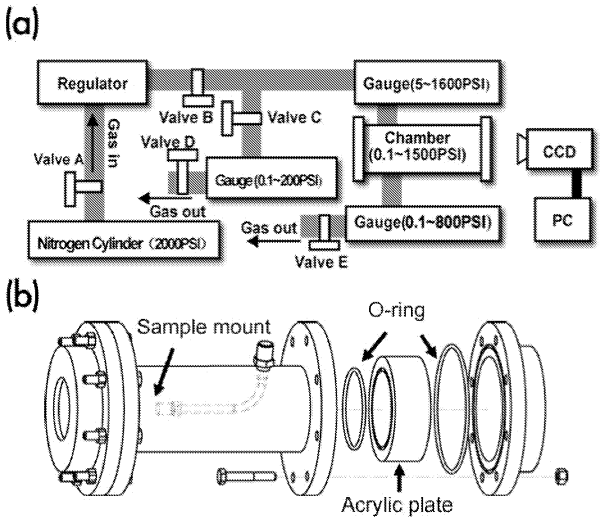

FIG. 1: (a) Schematic description of our experimental setup and (b) design of high-pressure chamber

TABLE I: Specifications of samples used in our experiment

No.	Material	$h_0(\mu$m)	Dimension(m)	number of sheets
1	Aluminum	16	0.15×0.15	1
2	Aluminum	32	0.15×0.15	1
3	Aluminum	16	0.15×0.075	2
4	Aluminum	16	0.15×0.05	3
5	Aluminum	16	0.20×0.20	1
6	HDPE	33	0.15×0.15	1
7	HDPE	33	0.30×0.30	1
8	HDPE	33	0.30×0.15	2

depends on the ball radius, we decide to switch back to the more direct P and replot the inset data as volume ratio, $D \equiv R_0^2 h_0/(4\pi R^3/3)$, versus P in Fig.2. The power-law $R/R_0 \propto 1/F^\alpha$ is still valid in the new scale, $D \propto P^{\alpha'}$ where $\alpha' = 3\alpha/(1+2\alpha)$. The deviation from power law implies that a different crumpling mechanism might be at work as the structure becomes more compact. Note that the density of the sample does not cease to grow even at pressure as large as 1.1×10^7Pa or equivalently a force of 450 kgw. As will be elaborated later, the high-pressure behavior in Fig.2 is quantitatively different from the jammed state predicted by [8] and surmised in [9].

The X-ray tomography[11] has confirmed that the interior of a crumpled ball develops separate domains of ordered layers at medium pressure. When a 2-D projection is taken on the big circles, the view resembles the lamellae phase of lyotropic liquid crystals. The data points that exhibit this phase fall in the transition region in Fig.2. This implies that the emergence of bundled layers may coincide with the demise of the power law. It is reasonable to conjecture then that the transition ends when the amorphous portion has been depleted by the

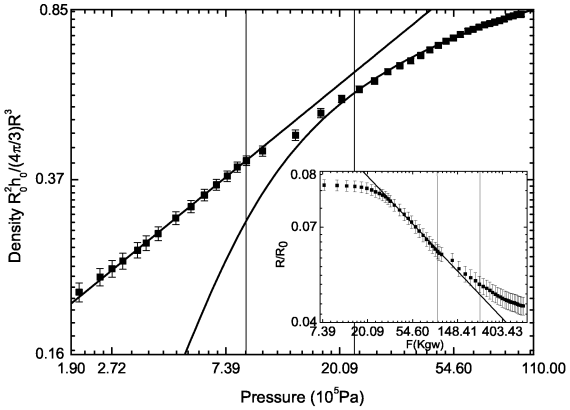

FIG. 2: The density is plotted against pressure for a single Al sheet with R_0=0.15×0.15m and $h_0 = 16\mu$m. The process can be divided into three regions. The two vertical lines mark the rough period when the power law transits smoothly to a scaling relation. Same data are plotted as R/R_0 vs F in the inset. The straight line is a guide to the eye, while the curved line at high pressure is a fitting by Eq.(5) with $\ell \simeq 1.55\mu$m and $\eta \simeq 2.3$, consistent with the X-ray data in Fig.3(b).

ordered domains. In other words, the first/third region in Fig.2 that exhibits the power-law/scaling behavior is a pure state of independent/bundled layers. In contrast, the transition region is a mixture of both states.

For elastic bending, the stress-strain relation can be expressed as $F/A = \kappa\theta$ where the constant A contains information of the width, length, and thickness h of the bundled layers and κ is the bending rigidity. When the strain θ exceeds the yield point θ_y, we assume that the stress-strain relation remains linear except the rigidity $\kappa' < \kappa$ becomes smaller due to the plasticity. Dividing

$$\frac{F}{A} = \kappa\theta_y + \kappa'(\theta - \theta_y) \tag{2}$$

by its derivative $d(F/A)/d\theta = \kappa'$, one obtains

$$\frac{d\theta}{d\ln F} = \theta + \theta_y\Big(\frac{\kappa}{\kappa'} - 1\Big). \tag{3}$$

Note that Eq.(3) describes the response of a single bundle. To shrink the ball by $-dR$, it involves many such bundles bent at different degrees. Since the bundle size roughly scales with the ball radius, it is reasonable to expect R to play the dominant length scale at bridging the averaged microscopic deformation $d\langle\theta\rangle$ and the macroscopic shrinkage: $R \times d\langle\theta\rangle = -dR$. On average, $\langle\theta\rangle$ roughly equals $\theta_s/2$ where θ_s is the maximum angle beyond which the bundle snaps and creates a new ridge:

$$-\frac{d\ln R}{d\ln F} = \frac{\theta_s}{2} + \theta_y\Big(\frac{\kappa}{\kappa'} - 1\Big). \tag{4}$$

Note that Eq.(4) can be equally applied to an elastic sheet by setting $\kappa' = \kappa$. A bent bundle is drawn schematically in Fig.3(a) to illustrate the largest elongation $\simeq h\theta$

happens at the upper layer. While the maximum extension ℓ a thin layer can withstand before snapping and converging all the potential energy to one singular line is a material property, we deduce $\theta_s \simeq \ell/h$.

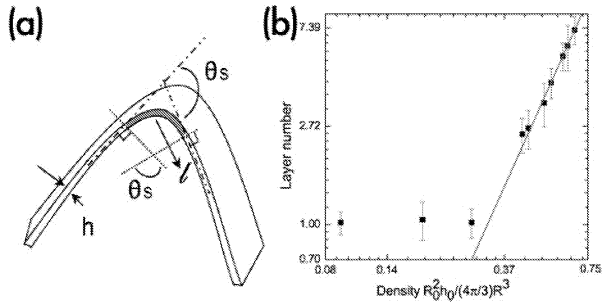

FIG. 3: (a) A bent plate is drawn to illustrate that the upper layer suffers an extension of $h\theta$. (b) From the X-ray tomography data[11] for Al, the increase of layer number in each domain can be fit by $h/h_0 \propto D^\eta$ at high densities with $\eta \simeq 2.3$.

Equation (4) gives a couple of predictions that are consistent with the experimental findings: (1) R/R_0 versus F obeys a power law if θ_s is a constant of R. We believe this is the case at low pressure since the layers have not yet bundled and $h = h_0$. (2) It is apparent how much angle a single layer can endure before snapping is an intrinsic property. So it is only natural that the exponent α is material-dependent[9]. (3) Imagine bending a straw or a fold sheet, the value of θ_s falls in the ball park of ten degrees, which translates to the right magnitude[9] of $\alpha \approx 0.1$. (4) Equation (4) predicts that plasticity enhances α since the second term is positive definite. This is consistent with the observation[9] that the Al foil exhibits a larger $\alpha \simeq 0.2$ than that of HDPE, $\alpha \simeq 0.1$. (5) When the layers start to align[11] at high pressure, the thickness of each bundle increases with the volume ratio (see Fig.3(b)). Since $\theta_s = \ell/h$, it is natural that the slope in the inset of Fig.2 or the α value gradually decreases further into the high-pressure region. (6) Aided by Fig.3(b), Eq.(4) can be expressed as an explicit ODE:

$$\frac{d\ln P}{d\ln D} \simeq \frac{2h_0 D^\eta}{3\ell} + \frac{2}{3} \tag{5}$$

where parameters ℓ and η distinguish different material. This is a strong prediction that there exists a scaling relation $P(D)$ for a partially-ordered compact elastic ball, independent of its thickness, size, and even scissoring. We shall present experimental proofs to validate Eq.(5).

The thickness and initial size are varied respectively in Fig.4 and the inset of Fig.5 for Al foils. In addition to demonstrating that the value of α is independent of these two parameters, both figures serve to illustrate why a plot in D-vs-P is more informative at high pressure than the conventional R/R_0-vs-F. Experimentally, the less complete collapse at low pressure is expected since α increases with the sheet number, see the triangle lines in Fig.5. Physically, this tells us that scissoring weakens

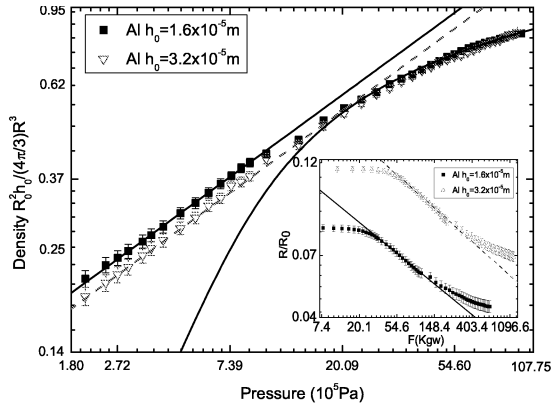

FIG. 4: (Color online) Same data in Fig.2 are used to compare with those with double thickness h_0=0.032mm but same R_0. The two data lines in the inset collapse to one in the main figure as we rescale the radius-vs-force to density-vs-pressure.

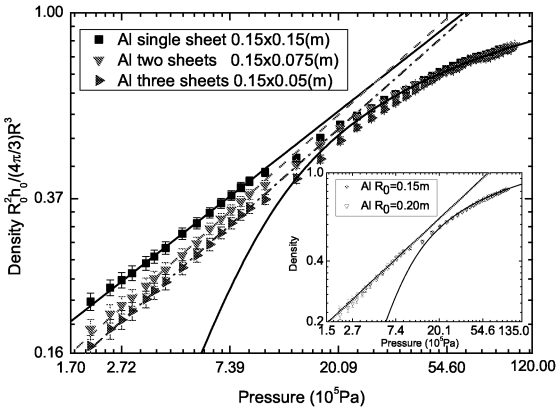

FIG. 5: (Color online) The data in Fig.2 for a single Al sheet of size 0.15×0.075m are plotted in contrast to those of double sheets of size 0.15m×0.075m and triple sheets of 0.15×0.05m. The α increases from 0.21 to 0.22 and 0.25 with the addition of sheets. Note how well these three lines collapse at high pressure. The inset shows data for single sheets of $h_0 = 0.016$mm but different initial sizes: $R_0 = 0.15$ and 0.20m.

the structure and renders the crumpled ball more compressible at low density and pressure. However, as the layers increase in number and start to bundle together at high pressure, the finite damage caused by the scissoring becomes relatively less important. In the face of external pressure, all it matters is the local density that determines its hardness and ability to resist.

In order to test the generalization of Eq.(5) for less plastic material, we changed the sample to HDPE. Figure 6 shows the data for two single sheets of different R_0 and double sheets. Same as Fig.5 for Al, the exponent α is independent of the initial size R_0, but increases from

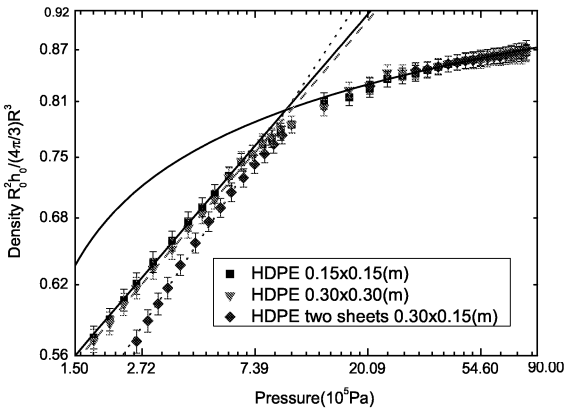

FIG. 6: (Color online) HDPE is used to show that the properties in Fig.5 are not unique to Al foils. The solid curve at high pressure is a fitting by Eq.(5) with $\eta \simeq 4.1$ and $\ell \simeq 2.7\mu$m.

0.10 to 0.13 for the double sheets. The gradual deviation from the power law at high pressure is once more obvious except the transition occurs at higher densities within roughly D =[72,85] as opposed to [40,58] for Al. The collapse is again more complete at high pressure.

Although we already glimpsed the sign of a transition away from the power-law behavior in a previous work[9], the reason why the high-pressure phase was mistaken for a jammed state was that (1) the acrylic-made chamber used in that study only allowed a maximum pressure of 160 PSI, in contrast to 1500 PSI in the current design. Therefore, the plateau feature at high pressure was less than a decade, which made the clarification of jamming or gradual decreasing difficult, (2) the sample tested in Ref.[9] was ten times larger than in this work. The turning at the jamming point was found to be sharper for larger samples perhaps due to the increase in layer number which made it easier to trap the configuration in a jammed state. Limited by the tiny space inside our high-pressure chamber, an examination of larger samples will need a complete remodeling. However, to continue this first-hand observation of the compact crumpled structure, further checks on the size dependence are necessary.

We have offered an intuitive argument for why α should increase for multiple sheets. Let's now understand it within the bundled-layer model: When crumpled sheets enter the power-law region, their facets are already considerably smaller than R_0, and it is unlikely that the scissoring will affect θ_s. So the difference must have entered from the mean-field, $\langle\theta\rangle$; i.e., the precise coefficient of θ_s in Eq.(4). Double sheets can be regarded as a single one with a line of chemical bonds or fibers removed. This apparently weakens the structure and will render shrinkage to the ball. However, a reduce in radius requires more layers to be bent. Consequently, the weighting of large angles for $\langle\theta\rangle$ should shift upwards. A logical question is why this argument fails at high pressures where the scaling relation in Eq.(5) has been demonstrated in Figs.5 and 6 to be insensitive to the sheet number. Isn't it true that the viscoelastic properties of polymer melts[13] remain sensitive to the polymer length? The answer is that this is a poor analogy since there are only two or three wiggling planes inside the crumpled ball. The finite damages from the scissoring are soon swamped by the huge number of layers when the ball is highly compact.

Sands and grains in a barn or silo also exhibit a nearly-jammed state in which crystallization can be promoted[14] by shearing or shaking. However, simply raising the stress level isotropically does not do much at inducing the ordering except making the granules jammed tighter and harder to flow. Furthermore, boundary conditions[14] have a more profound influence on the crystallization of the entire packing. Shear thickening in colloidal dispersions[15] is another case where the viscosity changes under shear stress. But, since it is a highly nonequilibrium, dissipative state, the accompanied order-disorder transition was believed to be less important[15].

In conclusion, we have designed a high-pressure chamber to study the nature of transition and the new state after the power-law behavior breaks down. A scaling relation between the volume ratio and pressure was deduced both empirically and theoretically for the high-pressure phase. We believe the emergence of ordered structure changes the mechanical response of the compact crumpled ball.

[1] T. A. Witten, Rev. Mod. Phys. **79**, 643 (2007).

[2] For instance, see P. A. Houle and J. P. Sethna, Phys. Rev. E **54**, 278 (1996); E. M. Kramer and T. A. Witten, Phys. Rev. Lett. **78**, 1303 (1997) for crumpling noises. And D. L. Blair and A. Kudrolli, Phys. Rev. Lett. **94**, 166107 (2005); C. A. Andresen *et al.*, Phys. Rev. E **76**, 026108 (2007) for topography on a crumpled sheet.

[3] T. Tallinen *et al.*, Phys. Rev. Lett. **105**, 026103 (2010); M. A. F. Gomes *et al.*, Phys. Rev. E **81**, 031127 (2010); A. S. Balankin *et al.*, Phys. Rev. E **81**, 061126 (2010).

[4] Y. Kantor, M. Kardar, and D. R. Nelson, Phys. Rev. Lett. **57**, 791 (1986).

[5] Kittiwit Matan *et al.*, Phys. Rev. Lett. **88**, 76101 (2002).

[6] G. A. Vliegenthart and G. Gompper, Nature Mater. **5**, 216 (2006).

[7] T. Tallinen *et al.*, Nature Mater. **8**, 25 (2009).

[8] Eric Sultan and Arezki Boudaoud, Phys. Rev. Lett. **96**, 136103 (2006).

[9] Y. C. Lin *et al.*, Phys. Rev. Lett. **101**, 125504 (2008).

[10] Y. C. Lin *et al.*, Phys. Rev. E **80**, 066114 (2009).

[11] Y. C. Lin *et al.*, Phys. Rev. Lett. **103**, 263902 (2009).

[12] Jacques Duran, *Sands, Powers, and Grains: An Introduction to the Physics of Granular Materials (Partially Ordered Systems)* (Springer-Verlag, NY, 1999).

[13] P. G. de Gennes, *Scaling Concepts in Polymers Physics* (Cornell University Press, Ithaca, NY, 1979).
[14] J. C. Tsai and J. P. Gollub, Phys. Rev. E **70**, 031303 (2004).
[15] N. J. Wagner and J. F. Brady, Phys. Today **62**, 27 (2009); H. M. Laun, Angew. Makromol. Chem. **123**, 335 (1984).